

**Keywords:** 5-hydroxymethylcytosine; epigenomic landscape; lncRNA; colorectal cancer; super-enhancer; prognosis biomarker

# Epigenomic landscape of 5-hydroxymethylcytosine reveals its transcriptional regulation of lncRNAs in colorectal cancer

Hanyang Hu<sup>1,3,6</sup>, Maoguo Shu<sup>2,6</sup>, Lin He<sup>2</sup>, Xueyuan Yu<sup>2</sup>, Xiangyu Liu<sup>2</sup>, Yalin Lu<sup>1</sup>, Yinghong Chen<sup>4</sup>, Xiaoping Miao<sup>5</sup> and Xiaohua Chen<sup>\*,1,3</sup>

<sup>1</sup>Department of Laboratory Medicine, No. 161 Hospital of PLA, Wuhan 430010, China; <sup>2</sup>Department of Plastic, Aesthetic and Craniofacial Surgery, The First Affiliated Hospital of Xi'an Jiaotong University, Xi'an 710061, China; <sup>3</sup>School of Basic Medical Science, Wuhan University, Wuhan, China; <sup>4</sup>Nursing Department, No. 161 Hospital of PLA, Wuhan 430010, China and <sup>5</sup>Department of Epidemiology and Biostatistics and the Ministry of Education Key Lab of Environment and Health, School of Public Health, Tongji Medical College, Huazhong University of Science and Technology, Wuhan, China

**Background:** DNA methylation at the 5 position of cytosine (5mC) can be converted to 5-hydroxymethylcytosine (5hmC) by the ten–eleven translocation family. The loss of global levels of 5hmC has been regarded as a hallmark in various cancers. 5-hydroxymethylcytosine is distributed at protein-coding gene bodies and promoters; however, the role and distribution of 5hmC at long non-coding RNAs (lncRNAs) is not clear. We investigated the distribution and regulatory roles of 5hmC for lncRNAs in colorectal cancer (CRC).

**Methods:** We integrated genome-wide profiles of 5hmC, 5mC, transcriptome and histone marks in CRC patients and examined the 5hmC-based clinical outcomes in patients.

**Results:** 5-hydroxymethylcytosine was distributed at lncRNA loci and positively correlated with lncRNA transcription. Dysregulated CRC lncRNAs were regulated by 5hmC directly or through abnormal activities of typical and super-enhancers and promoters modified by 5hmC. In addition, 5hmC was involved in long-range chromatin interactions at lncRNA loci. Finally, lncRNAs regulated by differential 5hmC marks were correlated with different clinical outcomes and tumour status in patients.

**Conclusions:** 5-hydroxymethylcytosine is critical in regulating the transcription of lncRNA and serve as novel biomarkers for clinical prognosis in CRC.

Colorectal cancer (CRC) is a major health problem associated with high morbidity and mortality worldwide (Jemal *et al*, 2011). Several critical genetic changes and pathways driving cancer initiation and progression have been uncovered, such as WNT, RAS, PI3K, TGF- $\beta$ , p53 and mismatch repair proteins (Fearon, 2011; Cancer Genome Atlas Network, 2012). Epigenetic abnormalities have also been explored and proved to be essential in the pathogenesis of cancer. For example, aberrant DNA methylation at the 5 position of cytosine (5mC) occurs extensively in many types of

cancer, exhibiting global hypomethylation and local hypermethylation at specific gene promoter CpG islands (Baylin and Jones, 2011; Dawson and Kouzarides, 2012). Such epigenetic changes were observed in CRC as well (Fearon, 2011; Vaiopoulos *et al*, 2014).

DNA methylation is dynamically regulated by DNA methyltransferases and the ten–eleven translocation (TET) family of 5mC hydroxylases. Ten–eleven translocation family proteins, including TET1, TET2 and TET3, can remove methylation in DNA and

\*Correspondence: Dr X Chen; E-mail: cxhniuniu@163.com

<sup>6</sup>These authors contributed equally to this work.

Received 13 June 2016; revised 10 December 2016; accepted 21 December 2016; published online 31 January 2017

© 2017 Cancer Research UK. All rights reserved 0007–0920/17

mediate the conversion of oxidised 5mC to 5-hydroxymethylcytosine (5hmC) in an  $\alpha$ -ketoglutarate- and Fe(II)-dependent manner (Tahiliani *et al*, 2009; Ito *et al*, 2010). Further oxidation of 5hmC generates 5-formylcytosine and 5-carboxylcytosine (He *et al*, 2011; Ito *et al*, 2011). Notably, 5hmC is most abundant in self-renewing cells, pluripotent stem cells and adult neural cells (Kriaucionis and Heintz, 2009; Szwagierczak *et al*, 2010). Recent genome-wide studies in embryonic stem cells and developing T cells have revealed that 5hmC was enriched in protein-coding gene bodies, promoters and cell-type-specific enhancers (Pastor *et al*, 2011; Stroud *et al*, 2011; Tsagaratou *et al*, 2014; Kim *et al*, 2014; Ichiyama *et al*, 2015). Cancers, however, exhibited strongly reduced 5hmC levels relative to the surrounding normal tissue (Jin *et al*, 2011). Several independent researchers have observed a reduction in global levels of 5hmC in CRC (Haffner *et al*, 2011; Li and Liu, 2011; Kudo *et al*, 2012; Zhang *et al*, 2013; Uribe-Lewis *et al*, 2015). However, the distribution of 5hmC at long non-coding RNAs (lncRNAs) remains to be elucidated.

Long non-coding RNA is longer than 200 nt and has little or no open reading frame. On the basis of the proximity between neighbouring transcripts, lncRNAs can be classified to five broad categories: sense, antisense, bidirectional, intronic and intergenic (Rinn and Chang, 2012). Accumulating evidence suggests that lncRNAs are involved in diverse physiological and pathological processes, such as cell growth, apoptosis, stem cell pluripotency, development and cancer biology (Guttman and Rinn, 2012; Ulitsky and Bartel, 2013; Hu *et al*, 2014). Epigenetic controls, such as DNA methylation (Yan *et al*, 2015) and histone modifications (Guttman *et al*, 2009; Prensner *et al*, 2011; Trimarchi *et al*, 2014; White *et al*, 2014), are essential for lncRNA transcription in cancers. Furthermore, the activities of enhancer- or promoter-affected transcription of some intergenic lncRNAs originate from these *cis*-elements (Marques *et al*, 2013).

To investigate the role of 5hmC in the transcriptional control of lncRNAs, we integrated genome-wide profiles of 5hmC, 5mC, transcriptome and several histone marks from patients with matched primary tumour and normal colon tissues. We showed that 5hmC was distributed at lncRNAs and positively correlated with lncRNA transcription. Dysregulated CRC lncRNAs were regulated by 5hmC directly or through abnormal activities of typical and super-enhancers and promoters modified by 5hmC. In addition, we found that 5hmC was involved in long-range chromatin interactions at lncRNA loci. Finally, lncRNAs regulated by differential 5hmC marks were correlated with different clinical outcomes and tumour status in patients. In conclusion, our findings revealed crucial roles for 5hmC in driving dysregulated transcriptional programmes of lncRNAs and contributed to the identification of novel biomarkers for prognosis evaluation in patients with CRC.

## MATERIALS AND METHODS

**Access to published data.** Publicly available hmeDIP-seq and matched input data files for CRC were obtained from GSE47590. Methylcap-seq data sets for CRC were obtained from GSE39068. H3K4me1, H3K4me3, H3K27ac and matched input ChIP-seq data sets for CRC were obtained from GSE36204. RNA-seq data sets for CRC were obtained from GSE50760. Pol II ChIP-seq data sets for HCT116 cells were obtained from GSE60106 and GSE47677. GRO-seq data sets for HCT116 cells were obtained from GSE38140. ChIA-PET data for HCT116 cells were obtained from GSE33664.

**hmeDIP-seq and methylcap-seq data processing.** Each of the raw hmeDIP-seq data sets for four matched tumour and normal tissue samples and respective input data, as well as methylcap-seq data for eight matched tumour and normal tissue samples, were aligned

to UCSC human genome build hg19 using Bowtie (Langmead *et al*, 2009). Duplicate reads were removed with picard-tools. Regions found to be enriched relative to input DNA were detected using the 'findPeaks' routine in HOMER (Heinz *et al*, 2010) with the 'histone' mode and default parameter values.

**ChIP-seq data processing.** Each of the raw H3K4me1, H3K4me3 and H3K27ac ChIP-seq data sets for tumour and normal tissue and input data was aligned to hg19 using Bowtie. Pol II ChIP-seq data sets for HCT116 cell were also aligned to hg19 using Bowtie. Enriched peaks or regions were identified by MACS (Zhang *et al*, 2008) and annotated by HOMER.

**GRO-seq data processing.** Three replicates of GRO-seq raw data for HCT116 colon cancer cells were aligned to hg19 using Bowtie. *De novo* transcript identification was performed using HOMER with the 'groseq' mode and default parameter values, which detected regions of continual GRO-Seq read coverage. For genome browse visualisation, the 'makeUCSCfile' command in HOMER was used to make a Bedgraph on each strand. The negative strand values were assigned negative values in the BedGraph file. The BedGraph values were then divided by the number of millions of mapped (309 772 394) reads to give values of reads per million per bp (RPM/bp) for each position in the genome. The two files (strands) were concatenated back together, and igvtools was used to create a TDF file for visualisation using the IGV browser (Robinson *et al*, 2011).

**RNA-sequencing data analysis.** All RNA-seq data were mapped to human reference genome hg19 using TopHat (Trapnell *et al*, 2009) with default parameters. The UCSC mRNA and lncRNA annotation files were merged into a single GTF file as a reference gene annotation file. The alignment BAM files were sorted and converted into SAM files with SAMtools, then subjected to read counting using the python package HTSeq (Anders *et al*, 2015). The read counts were converted into RPKM (Reads Per Kilobase of exon model per Million mapped reads).

**Differentially epigenetic mark enrichment analysis.** The alignment SAM files were converted into BAM files and sorted and indexed with SAMtools. Then the sorted BAM files were converted to BED files using BEDTools (Quinlan and Hall, 2010). diffReps (Shen *et al*, 2013) was used to quantitatively compare 5hmC, 5mC and H3K4me1 peaks in normal and tumour tissue using BED files. Peaks with FDR <0.05 and fold change >2 were considered as statistically significant.

**Bidirectional enhancer RNA (eRNA) detection and correlation with gene transcription.** For bidirectional eRNA analysis, we first searched the intergenic transcripts from GRO-seq. Paired eRNA peaks from opposite DNA strands were searched for, such that the plus strand peak centre had a greater genomic coordinate than the minus strand peak centre, and the distance between the 5' ends of the peak pair was <1 kb. Then the two start sites of a plus transcript and a minus transcript were paired together, and their midpoint was defined as the centre of a bidirectional transcript.

Lists of genes in 5hmC- and non-5hmC-marked eRNA-associated genes in tumour were obtained by downloading the region-gene association file for each class from GREAT. Duplicate gene names in two region-gene association files were discarded, then merged to the normalised expression data. Boxplots of log<sub>10</sub>-transformed GRO-seq counts and RPKM RNA-seq values for genes were then generated in R. Statistical significance between groups was assessed by the Wilcoxon rank-sum test.

**Patients and tissue samples.** To validate the expression of lncRNAs, we recruited six pairs of colorectal cancer tissue and corresponding non-tumour tissue samples, all of which were obtained from patients who underwent surgical operations at Hospital No. 161 in 2014. All the participants were histologically

confirmed to have colorectal cancer and did not receive any other therapy before enrolment. Informed consent was obtained from all the participants, and procedures used in this study were approved by the institutional review board at Hospital No. 161.

**RNA extraction and qRT-PCR.** All samples were immediately frozen with liquid nitrogen after surgical resection. Total RNA was isolated using Trizol Reagent (Invitrogen, Carlsbad, CA, USA). qPCR was performed using an iQ5 Real-Time PCR Detection System (Bio-Rad, Hercules, CA, USA) using SYBR Green Real-time PCR Master Mix (Toyobo Co., Ltd, Osaka, Japan) for the readout. All reactions were carried out in triplicate. Data were analysed using the  $2^{-\Delta\Delta CT}$  method.

## RESULTS

**Genome-wide distribution of 5hmC in CRC lncRNAs.** To explore the role of 5hmC in colon carcinogenesis, we analysed the hmeDIP-seq data from CRC patients (Uribe-Lewis *et al*, 2015). We also included methylcap-seq data sets that measure genome-wide 5mC for matched colon tumour and normal tissue (Simmer *et al*, 2012), as a direct comparison. In total, we identified 130 265

and 153 380 5hmC peaks, and 380 614 and 380 638 5mC peaks in tumour and normal colon. We first investigated the 5hmC distribution across long non-coding RNAs (lncRNAs) by plotting 5hmC and 5mC reads against UCSC lncRNAs across the whole gene body and 3 kb flanking regions distal to the TSS and TES. We showed that 5hmC was abundant at exons and depleted at the lncRNA TSSs but enriched at proximal sites downstream of TSSs and TESs in both tumour and normal colon (Figure 1A and B). The results showed a similar pattern for 5mC compared with 5hmC, except that the enrichment of 5mC at TSSs was observed in tumour (Figure 1A and B). The total number of peaks and read-density plot demonstrated a loss of 5hmC in tumour, which was consistent with the previously reported reduction of global levels of 5hmC in CRC (Haffner *et al*, 2011; Kudo *et al*, 2012). In contrast, 5mC modification levels in cancer and normal tissue seemed comparable, although a slight increase of 5mC in tumour was observed.

Notably, we found sets of lncRNAs showed different patterns for 5hmC and 5mC. These lncRNAs formed distinct clusters through the enrichment of 5hmC, enrichment of 5mC or binary marks of both 5hmC and 5mC (Figure 1A), indicating that different potentially active DNA demethylation processes occurred in these clusters of lncRNAs. In addition, we analysed the distribution of all the 5hmC and 5mC peaks in the human

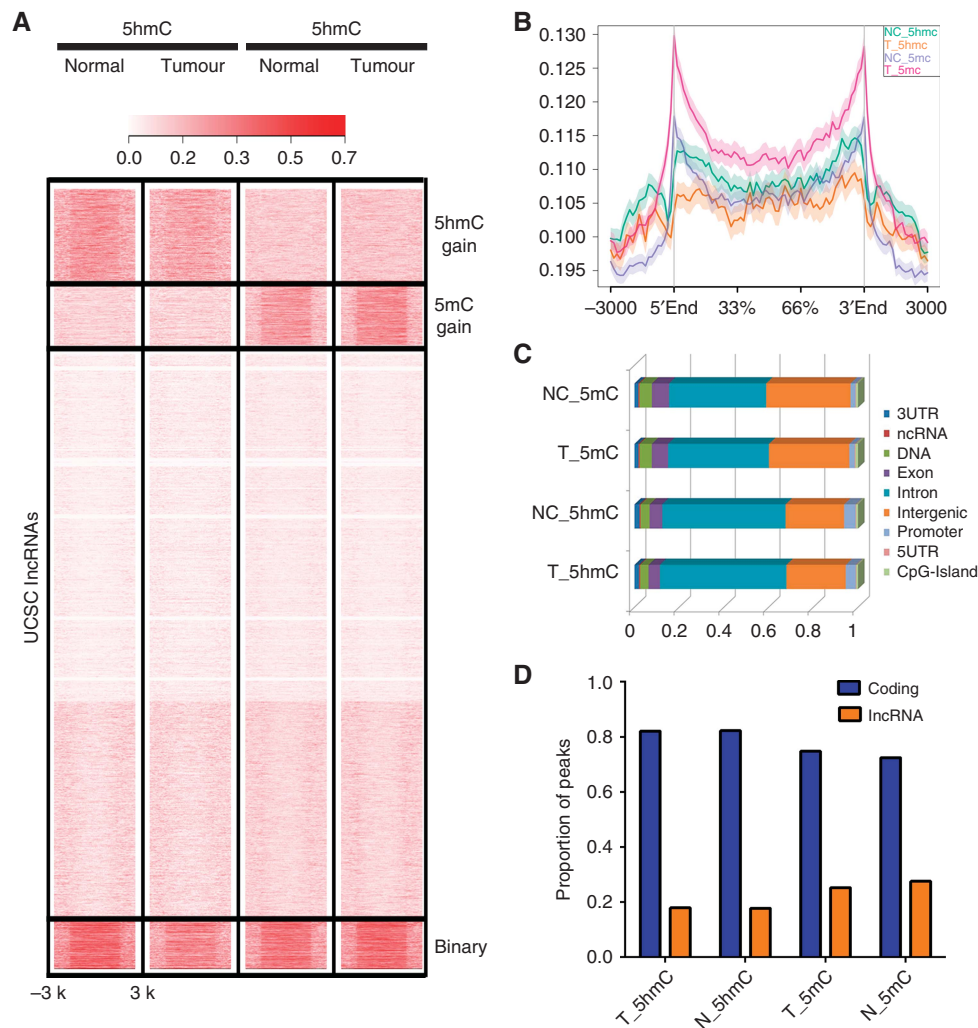


**Figure 1.** Comparison of genome-wide 5hmC and 5mC distribution in CRC lncRNAs. **(A)** Heat map representations of 5hmC and 5mC enrichment in UCSC lncRNAs across the whole gene body and 3 kb flanking region away from the TSS and TES. **(B)** The normalised tag density profiles for 5hmC and 5mC across lncRNA gene body ± 3 kb flanking regions with 200 bp resolution are shown. **(C)** The distribution of 5hmC and 5mC modifications was analysed on the basis of location: promoter (within 1 kb upstream from the transcription start site), exon, intron, intergenic, 3'UTR, 5'UTR, DNA, ncRNA and CpG-Island. **(D)** Distributions of 5hmC and 5mC between lncRNAs and protein-coding genes.



genome in nine kinds of regions: promoter, exon, intron, intergenic, 3'UTR, 5'UTR, DNA, ncRNA and CpG-Island. In addition to the enrichment at promoters and exons, the vast majority of 5hmC and 5mC peaks are distributed at intron and intergenic regions (Figure 1C). We also compared the distributions of 5hmC and 5mC between lncRNAs and protein-coding genes. As is shown in Figure 1D, about 18% of 5hmC peaks and 23% of 5mC peaks enriched at lncRNA loci, with no significant difference between tumour and normal tissue.

The majority of CpG dinucleotides are methylated, whereas unmethylated CpGs are found primarily in those regions of DNA with a relatively high density of CpG (CpG islands) in mammals. We therefore explored the distribution of 5hmC and 5mC among CpG islands. Our results showed that 5hmC was depleted at the centre of CGIs in both tumour and normal colon, whereas 5mC was enriched at the centre of CGIs but depleted at proximal upstream and downstream regions with respect to the centre in tumours (Supplementary Figure S1).

#### Abnormal 5hmC associated with colon cancer lncRNA signatures.

Although a global reduction was observed, locus-specific changes in 5hmC between tumour and normal colon remain unclear. Therefore, we set out to identify the differential modification of 5hmC regions in tumour relative to normal colon. In total, we found 1111 gain (up-5hmC) and 7687 loss (down-5hmC) sites (FDR <0.05 and fold change >2) in tumour (Figure 2A), reflecting the loss of 5hmC signal in CRC observed previously. For 5mC, we identified 4990 gain (up-5mC) and 3143 loss

(down-5mC) sites (FDR <0.05 and fold change >2; Figure 2A), suggesting that changes in DNA methylation were mild compared with 5hmC. Functional interpretations using the genomic regions enrichment of annotations tool (GREAT) revealed that gained 5hmC regions were associated with MSigDB Perturbation terms of COLON\_CANCER\_MSI\_UP, TP53\_TARGETS\_PHOSPHORYLATED and GRADE\_COLON\_CANCER\_UP (FDR <0.05). Disease ontology and phenotype enrichment analysis also suggested these regions were associated with colon adenocarcinoma and abnormal colon morphology (FDR <0.05). In contrast, down-5hmC sites revealed that these 5hmC loss regions were associated with several pathways involved in colon cancer progression, including MAPK, NOTCH, TGF-beta, WNT, PI3K and RAS signalling (FDR <0.05).

Transcription factors typically regulate gene expression by binding *cis*-acting regulatory elements, including promoters and enhancers, and recruiting co-activators and RNA polymerase II (RNA Pol II) to target genes. We next performed *de novo* motif analysis on the 5hmC gain and loss regions to identify the enriched sequence elements. This analysis revealed 5hmC gain regions were highly enriched for motifs recognised by TFs, including TEAD, JUNB, ERG, AHR and NR2E3 (Figure 2B). 5-hydroxymethylcytosin loss regions were also significantly enriched for several TF motifs, such as HIF1A, YY1, HNF6, MYCN and TFAP2C (Figure 2B).

Because studies have suggested that 5hmC at gene bodies is positively correlated with protein-coding gene expression, we herein set out to investigate the relationship between 5hmC

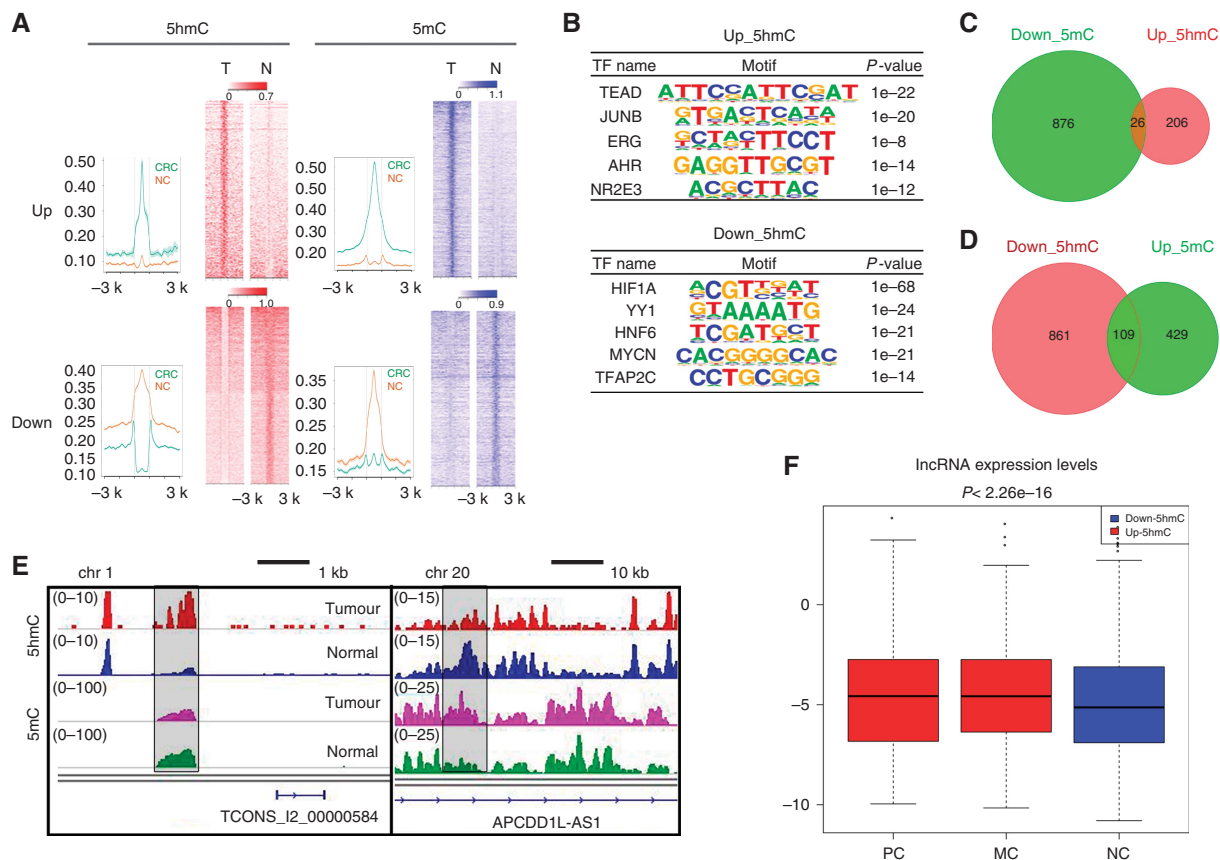


**Figure 2.** Differential modifications for 5hmC between tumour and normal colon. **(A)** Heat maps and the normalised tag density profiles show the differential modifications for 5hmC and 5mC between tumour and normal colon. **(B)** Top enriched transcription factor (TF) motifs identified by *de novo* motif discovery at gain-5hmC (upper panel) and loss-5hmC (lower panel) loci. **(C)** Venn diagram showing the number of up-5hmC containing lncRNAs marked by down-5mC. **(D)** Venn diagram showing the number of down-5hmC containing lncRNAs marked by up-5mC. **(E)** Examples of up-5hmC (left panel) marked and down-5hmC (right panel) marked lncRNAs. **(F)** Boxplots of log<sub>10</sub>-transformed (RPKM) gene expression values for gain-5hmC- and loss-5hmC-associated lncRNAs. P values were determined by Wilcoxon rank-sum test with continuity correction.

modification and lncRNA expression in colon cancer. By assigning the up-5hmC and down-5hmC peaks to their associated lncRNAs, we obtained 232 non-redundant lncRNAs marked with up-5hmC and 970 lncRNAs with down-5hmC (Supplementary Tables S1 and S2). Of these up-5hmC-associated lncRNAs, 26 also showed decreased 5mC levels, whereas 109 out of 970 down-5hmC-marked lncRNAs showed increased 5mC levels (Figure 2C and D). For example, upstream of TSS for *TCONS\_l2\_00000584* displayed a gain of 5hmC and a loss of 5mC (Figure 2E). In contrast, the *APCDD1L-AS1* locus showed a significant loss of 5hmC and gain of 5mC (Figure 2E). We analysed RNA-seq data (Kim *et al*, 2014b; Chen *et al*, 2016) in CRC to calculate expression levels for the up-5hmC and down-5hmC lncRNA list across normal, primary and liver metastatic cancer. Our results showed that up-5hmC-associated lncRNAs were expressed at a significantly higher level overall, relative to down-5hmC-associated lncRNAs ( $P < 2.26 \times 10^{-16}$ ; Figure 2F). Thus, our results demonstrated that 5hmC was correlated with higher lncRNA levels in CRC.

**Enrichment of 5hmC at typical and super-enhancers in colon cancer.** The enrichment of 5hmC at enhancers in embryonic stem cells (Yu *et al*, 2012) and developing T cells (Tsagaratou *et al*, 2014; Ichiyama *et al*, 2015) but not in NPC and neurons (Hahn *et al*, 2013) suggests that the genomic distribution of 5hmC is cell and tissue specific. Thus, we integrated our 5hmC and 5mC profiles with genome-wide profiles of H3K4me1 and H3K27ac, two histone modifications that mark enhancers, to explore the enrichment of 5hmC at enhancer regions. Heat maps of 5mC, H3K4me3, H3K4me1 and H3K27ac patterns within 3 kb surrounding the 5hmC peaks generated six distinct clusters (Figure 3A). Of these clusters, C4 and C6 indicated 5hmC-associated proximal promoters as areas of H3K4me3 co-occurrence. Importantly, we observed C3 representing 5hmC-marked distal enhancers, which exhibited highly enriched H3K4me1 and depleted H3K4me3 signals. In addition, this cluster was also enriched for H3K27ac, indicating that these enhancers can be further classified as active enhancers. We also found that 5mC was significantly depleted in these 5hmC-marked enhancers or promoters (Figure 3A and B). Collectively, these results suggest that 5hmC was enriched at active enhancers with 5mC depletion in CRC.

The fact that enrichment of 5hmC at typical enhancers promoted us to further investigate whether it also enriched at super-enhancers, which consists of multiple enhancers in close genomic proximity (Hnisz *et al*, 2013; Loven *et al*, 2013; Whyte *et al*, 2013). We extracted the colon cancer specific super-enhancers coordinates and mapped 5hmC and 5mC to these elements. We observed that super-enhancers were marked with 5hmC, with depletion of 5mC (Figure 3C and D), indicating that super-enhancers were possibly regulated by 5hmC.

Recent findings have indicated that CRC displayed thousands of locus-specific loss- or gain-of-H3K4me1 marks called variant enhancer loci (VELs) compared with normal colonic crypts (Akhtar-Zaidi *et al*, 2012). This specific feature leads us to ask if 5hmC is associated with these VELs. To address this, we identified 15 216 up-H3K4me1 and 23 215 down-H3K4me1 sites (FDR  $< 0.05$  and fold change  $> 2$ ) between tumour and normal colonic crypts. We therefore defined the up-H3K4me1 sites as gain VELs and the down-H3K4me1 sites as loss VELs. By mapping our 5hmC profiles against the VELs, we found that a fraction of both gain and loss VELs are marked by 5hmC and high levels of H3K27ac (Figure 3E and F). We observed that 5hmC levels in gain VELs are higher than those in loss VELs, whereas 5mC was depleted in gain VELs but enriched at loss VELs, suggesting that 5hmC is associated with enhancer activity.

Given that lncRNAs could arise from enhancer-associated or promoter-associated elements (Marques *et al*, 2013), we explored

the subclasses of lncRNAs regulated by 5hmC. We classified lncRNAs into enhancer- (elncRNA) and promoter-associated (plncRNA) groups according to chromatin status within 2 kb from each lncRNA TSS. As a result, 1513 lncRNAs were transcribed from 5hmC-marked enhancers, whereas 193 lncRNAs were from 5hmC-marked promoters. Further, we identified six lncRNAs associated with gain-5hmC-gain-VELs and one lncRNA associated with a gain-5hmC-gain promoter, whereas 15 lncRNAs were generated from loss-5hmC-loss-VELs and nine lncRNAs were generated from loss-5hmC-loss promoters. Taken together, these results indicated interaction between abnormal enhancer or promoter activities and that 5hmC modifications might drive dysregulated transcription of lncRNAs in CRC.

**5hmC-marked enhancers display higher activity than non-5hmC-marked enhancers.** Enhancers can also generate non-polyadenylated active bidirectional non-coding RNAs called enhancer RNAs (eRNAs) through the action of RNA polymerase II (pol II), which is considered a hallmark of functionally active enhancers (Lam *et al*, 2014). To characterise the regulatory relationship between 5hmC and eRNAs, we analysed genome-wide pol II binding and global nuclear run-on sequencing (GRO-seq) of nascent transcripts in colorectal cancer cells. First, we identified 32 821 intergenic H3K4me1 peaks, which we defined as intergenic enhancer loci. We then overlapped these intergenic enhancers with 5hmC profiles and obtained 8513 5hmC-marked and 25 215 non-5hmC-marked intergenic enhancers. After identifying pol II peaks and *de novo* transcripts, we found that 57 and 10.5% 5hmC-marked intergenic enhancers overlapped with at least one transcript and one pol II peak. In contrast, only 34 and 4.2% non-5hmC-marked intergenic enhancers overlapped with at least one transcript and one pol II peak.

Next, we identified 7763 intergenic bidirectional transcripts by searching both strands for paired peaks. We found that 5.2% 5hmC-marked intergenic enhancers and 4.7% non-5hmC-marked intergenic enhancers overlapped with those bidirectional transcripts, respectively. Although similar proportions of 5hmC-marked and non-5hmC-marked enhancers generating bidirectional transcripts were observed, we found that normalised GRO-seq read-density and pol II signals were more enriched at 5hmC-marked enhancers as compared with non-5hmC-marked enhancers (Figure 4A), suggesting that the transcriptional activity at 5hmC-marked enhancers was much higher than at non-5hmC-marked enhancers.

Given that eRNAs can promote the expression of proximal target genes (Kaikkonen *et al*, 2013; Lam *et al*, 2013; Li *et al*, 2013; Melo *et al*, 2013), we examined the transcriptional activity of putative target genes by quantifying the GRO-seq and RNA-sequencing (RNA-seq) read counts. Indeed, genes linked to higher eRNA production (Supplementary Table S3) at 5hmC-marked enhancers exhibited significantly higher GRO-seq and RNA-seq counts than genes linked to lower eRNA production (Supplementary Table S4) at non-5hmC enhancers (Figure 4B and C). Functional annotation of the genes targeted by 5hmC-associated eRNAs revealed that they were highly enriched for factors related to the immune process, cell cycle and signal transduction (Figure 4D). These genes were also implicated in critical signalling pathways closely related to colorectal cancer, including C-MYC, PI3K, NOTCH, P53 and WNT networks (Figure 4E). Collectively, our results indicated that enhancers marked with 5hmC displayed functional activity that might contribute to abnormal transcriptional programmes in colon cancer development.

**5hmC is involved in long-range chromatin interactions in CRC.** Higher-order chromosomal organisation represented by the physical interaction of promoters with distal regulatory elements is critical for transcriptional regulation. To test whether 5hmC is involved in chromatin interactions that regulate lncRNA

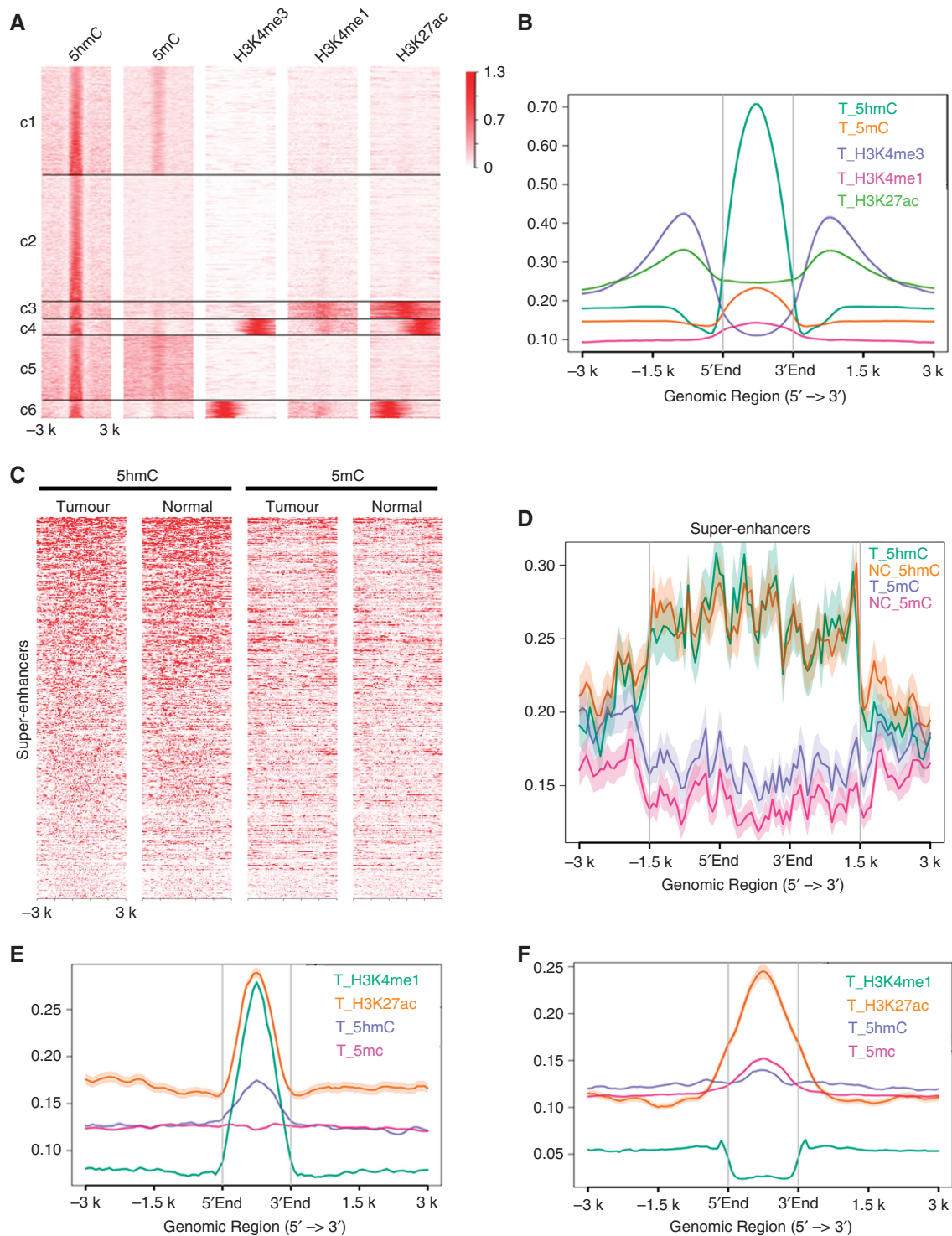


**Figure 3.** 5-hydroxymethylcytosine is enriched at enhancer regions in colon cancer. **(A)** Heat maps showing 5hmC, 5mC, H3K4me3, H3K4me1 and H3K27ac patterns within 3 kb surrounding the 5hmC peaks. **(B)** The normalised tag density profiles for 5hmC, 5mC, H3K4me3, H3K4me1 and H3K27ac within 3 kb surrounding the 5hmC peaks. **(C)** Heat maps showing 5hmC and 5mC patterns within 3 kb surrounding the colon cancer super-enhancers. **(D)** The normalised tag density profiles for 5hmC within 3 kb surrounding the 5hmC colon cancer super-enhancers. **(E, F)** The normalised tag density profiles for 5hmC, 5mC, H3K4me3, H3K4me1 and H3K27ac within 3 kb surrounding the gain VELS and loss VELS.

transcription, we analysed ChIA-PET data sets targeting RNA pol II in colorectal cancer cells (Li *et al*, 2012), which provided high resolution for the detection of long-range interactions on a global scale. RNA pol II-mediated long-range chromatin interactomes in colorectal cancer contained 19 264 clusters with both intra-chromosomal and interchromosomal interactions. Consistent with our hypothesis, 5hmC is highly enriched at these RNA pol II

interaction sites in CRC (Figure 5A and B). Interestingly, 5mC was enriched at these sites but showed much weaker signal levels than 5hmC (Figure 5B). In addition, loss of 5hmC and gain of 5mC in tumour as compared with normal tissue was examined at the interaction loci (Supplementary Figure S2). The results indicated that epigenetic changes may affect chromatin interactions contributing to abnormal transcriptional regulation in cancer.



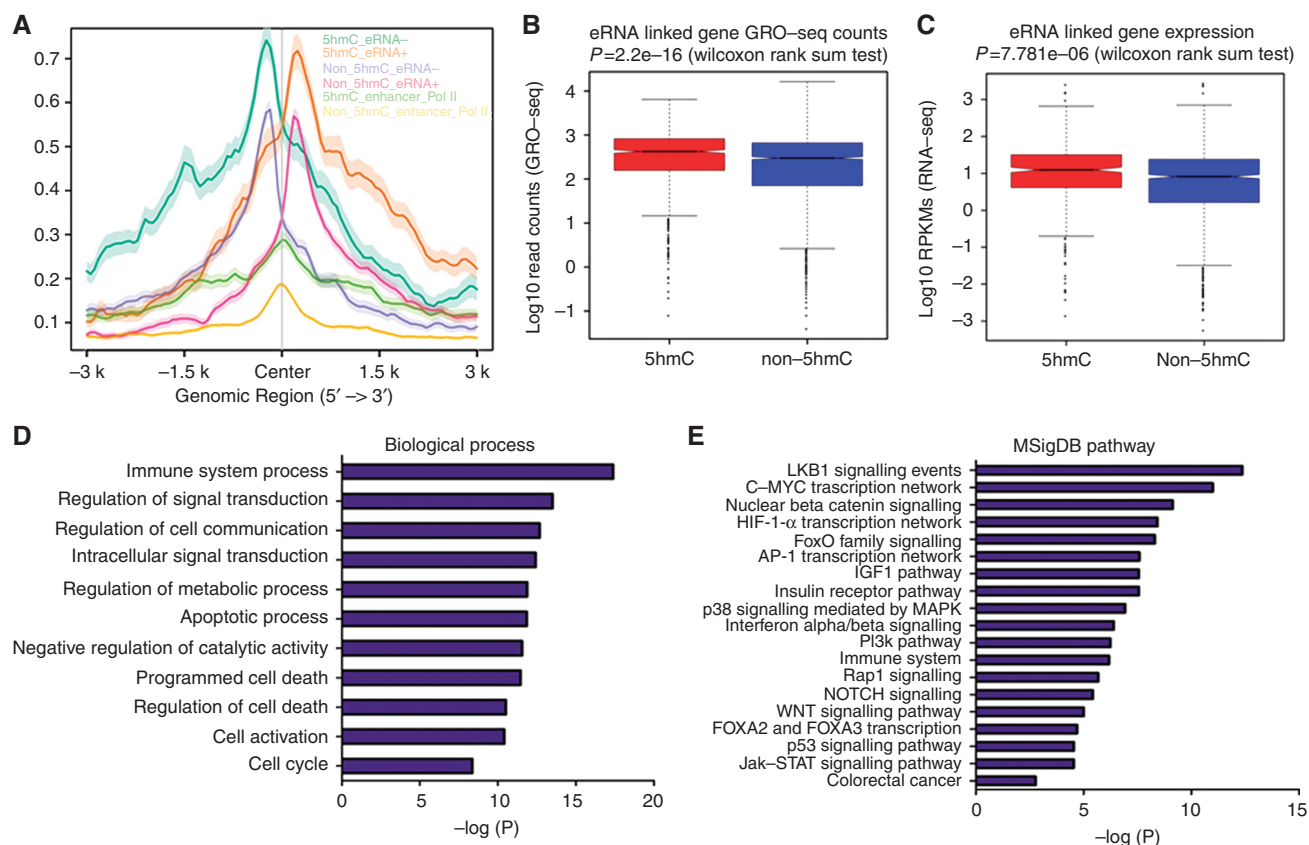


**Figure 4.** 5-hydroxymethylcytosine is positively correlated with enhancer activity. **(A)** Average GRO-Seq reads and normalised pol II tag density profiles at 5hmC- and non-5hmC-marked enhancer regions. **(B, C)** Boxplots of  $\log_{10}$ -transformed GRO-seq reads and RNA-seq expression values (RPKM) for 5hmC-marked enhancers related genes and non-5hmC-marked enhancers related genes. **(D, E)** Biological process and signalling pathways enrichment analysis for genes targeted by 5hmC-associated eRNAs.

We next explored the histone modifications to determine which marks participate in long-range interactions. We found the enrichment of several active histone modification marks at RNA pol II interaction sites, including H3K4me3, H3K4me1 and H3K27ac, confirming that the interactions were highly associated with actively transcribed promoters and distal enhancers, as reflected by the enrichment of GRO-seq reads at these loci (Figure 5B).

We further identified three types of interactions at lncRNA loci: enhancer-promoter, enhancer-enhancer and promoter-promoter interactions. All were associated with 5hmC and corresponding histone modification signatures (Figure 5C). For example, one enhancer-enhancer interaction involved an enhancer located upstream of *TCONS\_00016184* that interacted with another enhancer 30 kb downstream of *TCONS\_00016491*. Both the enhancers were marked by 5hmC and H3K4me1 and generated bidirectional transcripts. Furthermore, 5hmC was involved in promoter-promoter and promoter-enhancer interactions, as exemplified by observations that the promoter of *TCONS\_00009259* interacted with the promoter of coding gene *PHF15* and that the promoter of *TCONS\_l2\_00023557* interacted with the enhancer located within its intron. Interacting promoters and enhancers show high levels of transcriptional activity, as reflected by active histone mark occupation and transcription. Collectively, these observations suggest that 5hmC, together with several histone marks and transcription factors, established open chromatin structures that facilitate chromatin interactions that regulate lncRNA transcription.

**Prognosis associated with lncRNAs regulated by 5hmC.** To evaluate the clinical significance of dysregulated 5hmC, we next set

out to determine the expressions of the 1202 lncRNAs marked with the gain or loss of 5hmC. We first explored the expression patterns of these lncRNAs using RNA-seq data. This allowed us to distinguish primary, metastatic and normal samples (Figure 6A). We also validated the expression of six lncRNAs in our six matched CRC samples using qPCR (Figure 6B), the results of which were consistent with 5hmC modification status.

We then examined the prognostic value of those lncRNA signatures for TCGA through TANRIC (Li *et al.*, 2015). Higher expression of gain-5hmC-marked lncRNA, *LINC00189*, was significantly correlated with poor overall patient survival (Figure 6C). We also observed the expression of another lncRNA, *ENSG00000182165.13*, was correlated with microsatellite instability (MSI; Figure 6D). In contrast, lower expression of loss-5hmC-marked lncRNA, *LOC286297*, was significantly correlated with poor overall patient survival (Figure 6E). The expression of *ENSG00000223561.2* was correlated with tumour stage (Figure 6F). Taken together, these results suggest that lncRNAs had predictive and prognostic value in the management of CRC.

## DISCUSSION

Recent studies have shown that the global loss of 5hmC is a hallmark of various cancers, suggesting a potential role for 5hmC-mediated epigenetic regulation in cancer biology. Although genome-wide 5hmC maps have been generated for several cell types, the functional role of 5hmC remains limited. In this study, we systemically investigated the genome-wide patterns and functional relevance of 5hmC by integrating data resources, including 5hmC, transcriptome data, chromatin interactome data

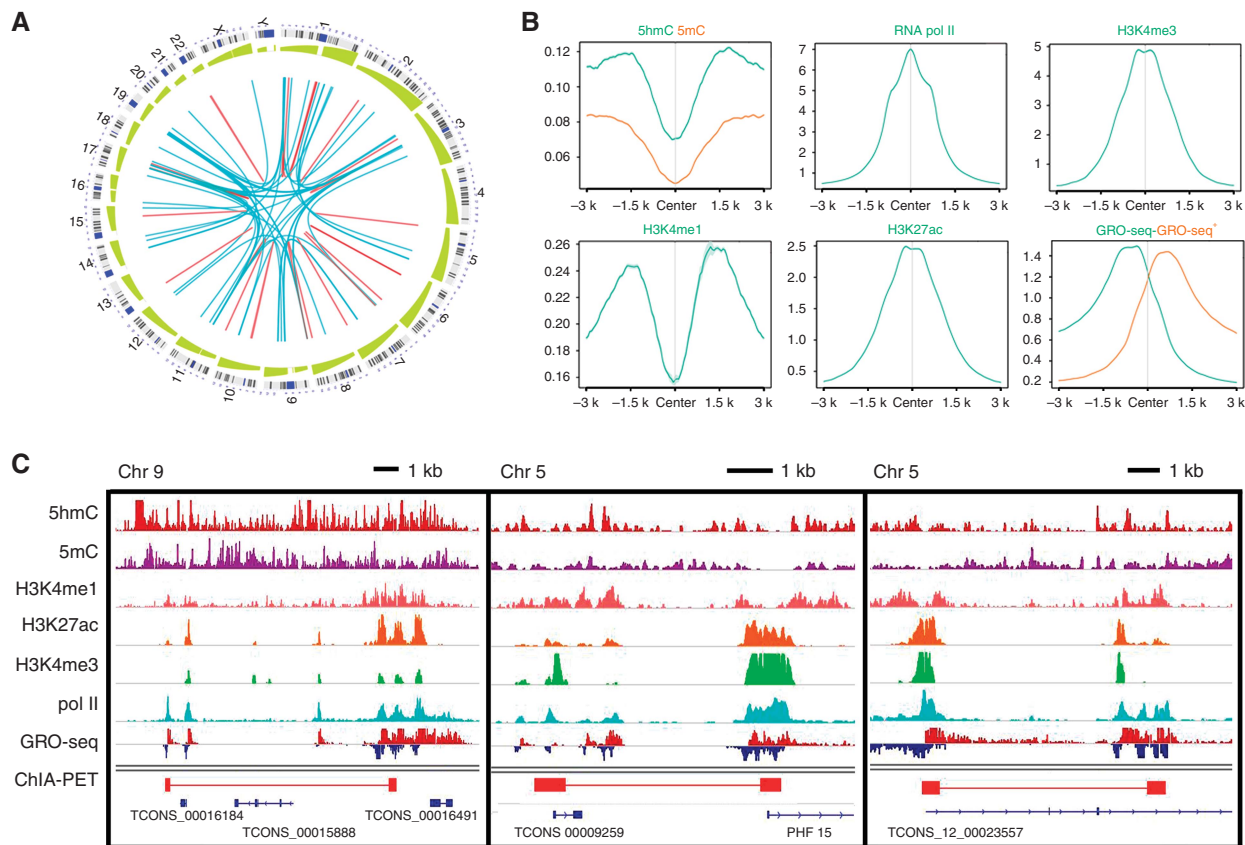


**Figure 5.** 5-hydroxymethylcytosine is involved in RNA pol II-mediated chromatin interactome. **(A)** Circos map of the whole-genome pol II chromatin interactome (Interaction PET count >7) and 5hmC occupancies from chromosome 1 to chromosome X, generated using the OmicCircos package. Interactions are drawn in the innermost ring, followed by the 5hmC track (green) that shows the peak signals of 5hmC. Interchromosomal interactions are drawn with blue and intrachromosomal interactions are drawn with red. **(B)** The normalised tag density profiles for 5hmC, pol II, 5mC, H3K4me3, H3K4me1, H3K27ac and GRO-seq reads at chromatin interaction sites defined by ChIA-PET peaks. **(C)** Example showing enhancer–enhancer (left panel), promoter–promoter (middle panel) and promoter–enhancer (right panel) interaction at the lncRNA loci.

and several histone modifications. We provided the first report that in addition to previously reported protein-coding genes, 5hmC was also distributed at lncRNA loci and correlated with dysregulated lncRNAs. These findings together extend our knowledge about the epigenetic regulatory roles of 5hmC and *cis*-regulatory elements for controlling transcription in CRC.

Polyadenylated lncRNA is transcribed by RNA pol II and associated with epigenetic signatures that are common to protein-coding genes, such as H3K4me3, at the promoter and H3K36me3 throughout the gene body (Guttman *et al*, 2009). Previous work has shown enriched H3K4me3 at the TSS of lncRNA genes in cancers, including T-ALL, prostate cancer and lung cancer (Prensner *et al*, 2011; Trimarchi *et al*, 2014; White *et al*, 2014). Thus, our novel discovery that lncRNAs showed similar patterns to those of protein-coding genes in 5hmC distributions further indicated that lncRNAs share certain epigenetic control mechanisms with protein-coding genes. However, we observed that the average 5hmC signal for lncRNAs was lower than that observed for coding genes. As 5hmC at gene body is positively correlated with transcription, we suggest that the observation in previous studies that lncRNA was less actively transcribed than mRNA (Cabili *et al*, 2011; Trimarchi *et al*, 2014) could be partially explained by the lower-average 5hmC signal for lncRNAs.

We characterised thousands of locus-specific gain or loss of 5hmC regions, which were implicated in several pathways and transcription factor occupancy. TEAD family transcription factors, overrepresented in gain-5hmC regions, are the major intracellular mediators of the Hippo–Yap pathway and TEAD–AP1 cooperation

drives the expression of a unique core set of target genes, thereby directing cancer cell migration and invasion (Liu *et al*, 2016). Thus, we suggested that lncRNAs associated with the gain or loss 5hmC regions might be members of those signalling and regulated by the transcription factor.

To evaluate the clinical significance of differential modifications of 5hmC, we examined their associated lncRNA expression patterns in primary, metastatic tumour and normal colon. We showed that these lncRNAs exhibited distinct expression patterns in cancerous and normal tissue, whereas some metastatic tumours were similar to primary tumours with lncRNA expression changes, reflecting 5hmC changes across various tumour status. To further examine these lncRNA signatures in TCGA data using TANRIC, we mapped our lncRNAs to GENCODE V19 annotations. Among the mapped lncRNAs, some lncRNAs were correlated with distinct overall survival outcomes, tumour stage and MSI status. Thus, 5hmC as well as associated lncRNA signatures might serve as new diagnostic and prognostic prediction markers in CRC.

It has been suggested that several variants in LD could impact multiple enhancers and cooperatively affect target gene expression (Corradin *et al*, 2014). Here we obtained a list of the colon cancer-associated variant set, which included 18 clusters with 18 risk-associated SNPs and 568 linked SNPs that were in LD with each of the risk-associated SNPs. Of the 586 SNPs, 7.7% (45) were significantly mapped to 5hmC-marked regions ( $P=0.001$ ), including 15 clusters. In addition, the vast majority of the remaining SNPs were located less than 10 kb from 5hmC regions. We also found that 5hmC regions containing SNPs exhibited a



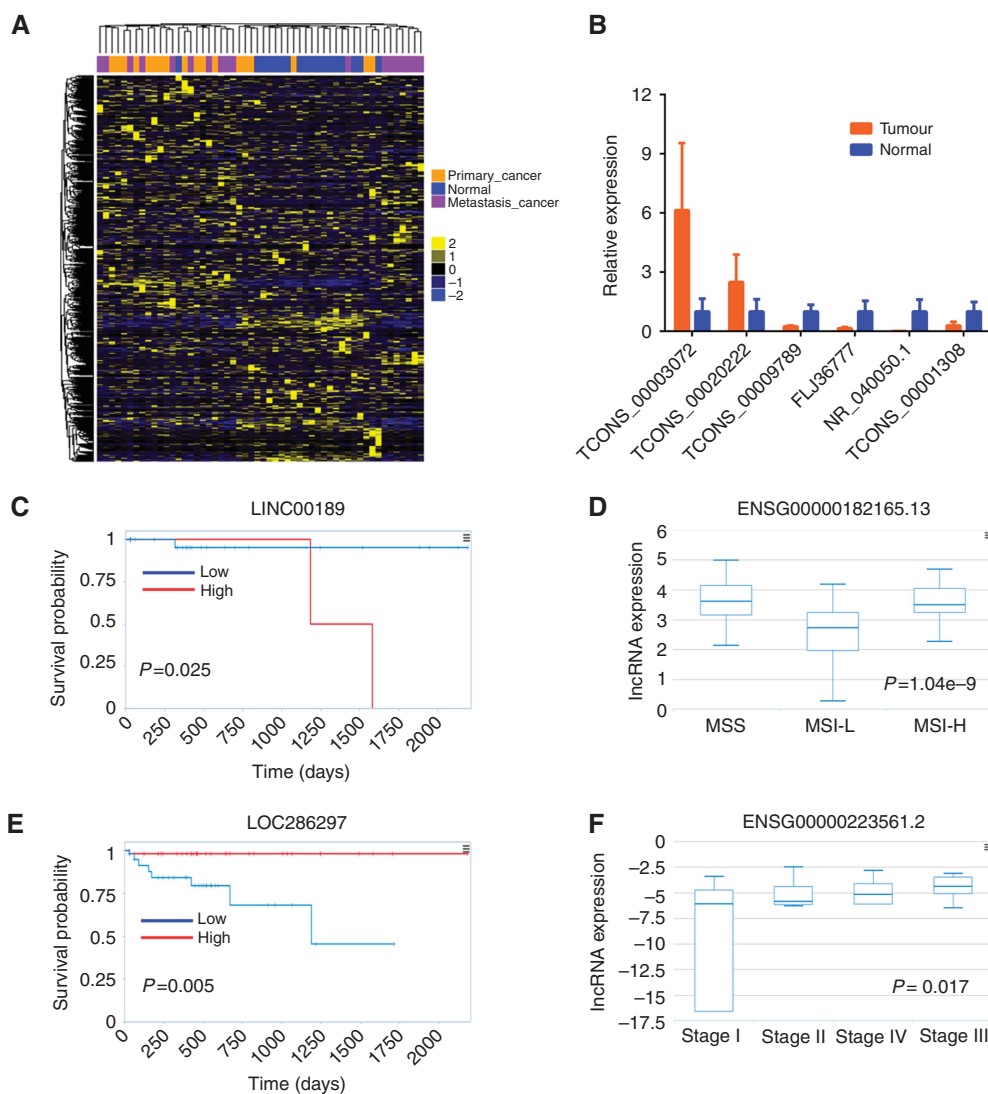


**Figure 6.** Clinical evaluation of 5hmC-associated lncRNAs. **(A)** Heat map of lncRNAs expression pattern in primary, metastasis and normal colon. **(B)** qPCR validation of the differential 5hmC-associated lncRNAs. Replicates ( $n=6$ ) of each sample were run and the Ct values averaged. All Ct values were normalised to  $\beta$ -actin. **(C)** Kaplan–Meier curves for overall survival time in patients with CRC according to expression of *LINC00189*. **(D)** Boxplot for MSI status in patients with CRC according to expression of *ENSG00000182165.13*. **(E)** Kaplan–Meier curves for overall survival time in patients with CRC according to expression of *LOC286297*. **(F)** Boxplot for tumour stage in patients with CRC according to expression of *ENSG00000223561.2*.

higher 5hmC signal level than control 5hmC sites not associated with colon cancer SNPs. We speculate that non-coding GWAS variants located within these types of enhancers could modulate gene expression, in some way, by affecting 5hmC-regulated enhancer activity. Notably, we also found CRC variants that mapped to a single 5hmC-marked enhancer at the *SMAD7* locus, which contains a super-enhancer in CRC (Hnisz *et al*, 2013). A super-enhancer comprises large enhancer clusters that control cell identity (Hnisz *et al*, 2013; Whyte *et al*, 2013), can be defined by histone H3K27ac modification, and is associated with key oncogenes in several cancer cell types (Hnisz *et al*, 2013; Loven *et al*, 2013). In CRC, many cancer hallmark genes that function in the multistep process of tumour pathogenesis acquired super-enhancers (Hnisz *et al*, 2013). As a fraction of super-enhancers were occupied by 5hmC, we suggest that 5hmC is involved in the process of tumour pathogenesis driven by super-enhancers.

In conclusion, we have systemically investigated the genome-wide patterns and functional relevance of 5hmC in CRC. Our findings suggest potential roles for 5hmC in the regulation of

tumour-specific promoters, enhancers and lncRNAs, thereby contributing to the pathogenesis of CRC, which will need to be taken into consideration in future studies of oncogenic transcriptional control in CRC.

## ACKNOWLEDGEMENTS

We thank the respective authors for their contributions to generate the sequencing data, as well as all the people who participated in this study and helped us successfully complete the research. This work was supported by the National Natural Science Foundation of China (Grant No. 81372077).

## CONFLICT OF INTEREST

The authors declare no conflict of interest.

## REFERENCES

- Akhtar-Zaidi B, Cowper-Sal-lari R, Corradin O, Saiakhova A, Bartels CF, Balasubramanian D, Myeroff L, Lutterbaugh J, Jarrar A, Kalady MF, Willis J, Moore JH, Tesar PJ, Laframboise T, Markowitz S, Lupien M, Scacheri PC (2012) Epigenomic enhancer profiling defines a signature of colon cancer. *Science* **336**(6082): 736–739.
- Anders S, Pyl PT, Huber W (2015) HTSeq—a Python framework to work with high-throughput sequencing data. *Bioinformatics* **31**(2): 166–169.
- Baylin SB, Jones PA (2011) A decade of exploring the cancer epigenome—biological and translational implications. *Nat Rev Cancer* **11**(10): 726–734.
- Cabili MN, Trapnell C, Goff L, Koziol M, Tazon-Vega B, Regev A, Rinn JL (2011) Integrative annotation of human large intergenic noncoding RNAs reveals global properties and specific subclasses. *Genes Dev* **25**(18): 1915–1927.
- Cancer Genome Atlas Network (2012) Comprehensive molecular characterization of human colon and rectal cancer. *Nature* **487**(7407): 330–337.
- Chen X, Liu B, Yang R, Guo Y, Li F, Wang L, Hu H (2016) Integrated analysis of long non-coding RNAs in human colorectal cancer. *Oncotarget* **7**(17): 23897–23908.
- Corradin O, Saiakhova A, Akhtar-Zaidi B, Myeroff L, Willis J, Cowper-Sal lari R, Lupien M, Markowitz S, Scacheri PC (2014) Combinatorial effects of multiple enhancer variants in linkage disequilibrium dictate levels of gene expression to confer susceptibility to common traits. *Genome Res* **24**(1): 1–13.
- Dawson MA, Kouzarides T (2012) Cancer epigenetics: from mechanism to therapy. *Cell* **150**(1): 12–27.
- Fearon ER (2011) Molecular genetics of colorectal cancer. *Annu Rev Pathol* **6**: 479–507.
- Guttman M, Amit I, Garber M, French C, Lin MF, Feldser D, Huarte M, Zuk O, Carey BW, Cassady JP, Cabili MN, Jaenisch R, Mikkelsen TS, Jacks T, Hacohen N, Bernstein BE, Kellis M, Regev A, Rinn JL, Lander ES (2009) Chromatin signature reveals over a thousand highly conserved large non-coding RNAs in mammals. *Nature* **458**(7235): 223–227.
- Guttman M, Rinn JL (2012) Modular regulatory principles of large non-coding RNAs. *Nature* **482**(7385): 339–346.
- Haffner MC, Chau A, Meeker AK, Esopi DM, Gerber J, Pellakuru LG, Toubaji A, Argani P, Iacobuzio-Donahue C, Nelson WG, Netto GJ, De Marzo AM, Yegnasubramanian S (2011) Global 5-hydroxymethylcytosine content is significantly reduced in tissue stem/progenitor cell compartments and in human cancers. *Oncotarget* **2**(8): 627–637.
- Hahn MA, Qiu R, Wu X, Li AX, Zhang H, Wang J, Jui J, Jin SG, Jiang Y, Pfeifer GP, Lu Q (2013) Dynamics of 5-hydroxymethylcytosine and chromatin marks in mammalian neurogenesis. *Cell Rep* **3**(2): 291–300.
- He YF, Li BZ, Li Z, Liu P, Wang Y, Tang Q, Ding J, Jia Y, Chen Z, Li L, Sun Y, Li X, Dai Q, Song CX, Zhang K, He C, Xu GL (2011) Tet-mediated formation of 5-carboxylcytosine and its excision by TDG in mammalian DNA. *Science* **333**(6047): 1303–1307.
- Heinz S, Benner C, Spann N, Bertolino E, Lin YC, Laslo P, Cheng JX, Murre C, Singh H, Glass CK (2010) Simple combinations of lineage-determining transcription factors prime cis-regulatory elements required for macrophage and B cell identities. *Mol Cell* **38**(4): 576–589.
- Hnisz D, Abraham BJ, Lee TI, Lau A, Saint-Andre V, Sigova AA, Hoke HA, Young RA (2013) Super-enhancers in the control of cell identity and disease. *Cell* **155**(4): 934–947.
- Hu Y, Chen HY, Yu CY, Xu J, Wang JL, Qian J, Zhang X, Fang JY (2014) A long non-coding RNA signature to improve prognosis prediction of colorectal cancer. *Oncotarget* **5**(8): 2230–2242.
- Ichihama K, Chen T, Wang X, Yan X, Kim BS, Tanaka S, Ndiaye-Lobry D, Deng Y, Zou Y, Zheng P, Tian Q, Aifantis I, Wei L, Dong C (2015) The methylcytosine dioxygenase tet2 promotes DNA demethylation and activation of cytokine gene expression in T cells. *Immunity* **42**(4): 613–626.
- Ito S, D'Alessio AC, Taranova OV, Hong K, Sowers LC, Zhang Y (2010) Role of Tet proteins in 5mC to 5hmC conversion, ES-cell self-renewal and inner cell mass specification. *Nature* **466**(7310): 1129–1133.
- Ito S, Shen L, Dai Q, Wu SC, Collins LB, Swenberg JA, He C, Zhang Y (2011) Tet proteins can convert 5-methylcytosine to 5-formylcytosine and 5-carboxylcytosine. *Science* **333**(6047): 1300–1303.
- Jemal A, Bray F, Center MM, Ferlay J, Ward E, Forman D (2011) Global cancer statistics. *CA Cancer J Clin* **61**(2): 69–90.
- Jin SG, Jiang Y, Qiu R, Rauch TA, Wang Y, Schackert G, Krex D, Lu Q, Pfeifer GP (2011) 5-Hydroxymethylcytosine is strongly depleted in human cancers but its levels do not correlate with IDH1 mutations. *Cancer Res* **71**(24): 7360–7365.
- Kaikkonen MU, Spann NJ, Heinz S, Romanoski CE, Allison KA, Stender JD, Chun HB, Tough DF, Prinjha RK, Benner C, Glass CK (2013) Remodeling of the enhancer landscape during macrophage activation is coupled to enhancer transcription. *Mol Cell* **51**(3): 310–325.
- Kim M, Park YK, Kang TW, Lee SH, Rhee YH, Park JL, Kim HJ, Lee D, Kim SY, Kim YS (2014a) Dynamic changes in DNA methylation and hydroxymethylation when hES cells undergo differentiation toward a neuronal lineage. *Hum Mol Genet* **23**(3): 657–667.
- Kim SK, Kim SY, Kim JH, Roh SA, Cho DH, Kim YS, Kim JC (2014b) A nineteen gene-based risk score classifier predicts prognosis of colorectal cancer patients. *Mol Oncol* **8**(8): 1653–1666.
- Kriaucionis S, Heintz N (2009) The nuclear DNA base 5-hydroxymethylcytosine is present in Purkinje neurons and the brain. *Science* **324**(5929): 929–930.
- Kudo Y, Tateishi K, Yamamoto K, Yamamoto S, Asaoka Y, Ijichi H, Nagae G, Yoshida H, Aburatani H, Koike K (2012) Loss of 5-hydroxymethylcytosine is accompanied with malignant cellular transformation. *Cancer Sci* **103**(4): 670–676.
- Lam MT, Cho H, Lesch HP, Gosselin D, Heinz S, Tanaka-Oishi Y, Benner C, Kaikkonen MU, Kim AS, Kosaka M, Lee CY, Watt A, Grossman TR, Rosenfeld MG, Evans RM, Glass CK (2013) Rev-Erbs repress macrophage gene expression by inhibiting enhancer-directed transcription. *Nature* **498**(7455): 511–515.
- Lam MT, Li W, Rosenfeld MG, Glass CK (2014) Enhancer RNAs and regulated transcriptional programs. *Trends Biochem Sci* **39**(4): 170–182.
- Langmead B, Trapnell C, Pop M, Salzberg SL (2009) Ultrafast and memory-efficient alignment of short DNA sequences to the human genome. *Genome Biol* **10**(3): R25.
- Li G, Ruan X, Auerbach RK, Sandhu KS, Zheng M, Wang P, Poh HM, Goh Y, Lim J, Zhang J, Sim HS, Peh SQ, Mulawadi FH, Ong CT, Orlov YL, Hong S, Zhang Z, Landt S, Raha D, Euskirchen G, Wei CL, Ge W, Wang H, Davis C, Fisher-Aylor KI, Mortazavi A, Gerstein M, Gingeras T, Wold B, Sun Y, Fullwood MJ, Cheung E, Liu E, Sung WK, Snyder M, Ruan Y (2012) Extensive promoter-centered chromatin interactions provide a topological basis for transcription regulation. *Cell* **148**(1–2): 84–98.
- Li J, Han L, Roebuck P, Diao L, Liu L, Yuan Y, Weinstein JN, Liang H (2015) TANRIC: an interactive open platform to explore the function of lncRNAs in cancer. *Cancer Res* **75**(18): 3728–3737.
- Li W, Liu M (2011) Distribution of 5-hydroxymethylcytosine in different human tissues. *J Nucleic Acids* **2011**: 870726.
- Li W, Notani D, Ma Q, Tanasa B, Nunez E, Chen AY, Merkurjev D, Zhang J, Ohgi K, Song X, Oh S, Kim HS, Glass CK, Rosenfeld MG (2013) Functional roles of enhancer RNAs for oestrogen-dependent transcriptional activation. *Nature* **498**(7455): 516–520.
- Liu X, Li H, Rajurkar M, Li Q, Cotton JL, Ou J, Zhu LJ, Goel HL, Mercurio AM, Park JS, Davis RJ, Mao J (2016) Tead and API coordinate transcription and motility. *Cell Rep* **14**(5): 1169–1180.
- Loven J, Hoke HA, Lin CY, Lau A, Orlando DA, Vakoc CR, Bradner JE, Lee TI, Young RA (2013) Selective inhibition of tumor oncogenes by disruption of super-enhancers. *Cell* **153**(2): 320–334.
- Marques AC, Hughes J, Graham B, Kowalczyk MS, Higgs DR, Ponting CP (2013) Chromatin signatures at transcriptional start sites separate two equally populated yet distinct classes of intergenic long noncoding RNAs. *Genome Biol* **14**(11): R131.
- Melo CA, Drost J, Wijchers PJ, van de Werken H, de Wit E, Oude Vrielink JA, Elkon R, Melo SA, Leveille N, Kalluri R, de Laat W, Agami R (2013) eRNAs are required for p53-dependent enhancer activity and gene transcription. *Mol Cell* **49**(3): 524–535.
- Pastor WA, Pape UJ, Huang Y, Henderson HR, Lister R, Ko M, McLoughlin EM, Brudno Y, Mahapatra S, Kapranov P, Tahiliani M, Daley GQ, Liu XS, Ecker JR, Milos PM, Agarwal S, Rao A (2011) Genome-wide mapping of 5-hydroxymethylcytosine in embryonic stem cells. *Nature* **473**(7347): 394–397.
- Prensner JR, Iyer MK, Balbin OA, Dhanasekaran SM, Cao Q, Brenner JC, Laxman B, Asangani IA, Grasso CS, Kominsky HD, Cao X, Jing X, Wang X, Siddiqui J, Wei JT, Robinson D, Iyer HK, Palanisamy N, Maher CA, Chinnaiyan AM (2011) Transcriptome sequencing across a prostate cancer cohort identifies PCAT-1, an unannotated lincRNA implicated in disease progression. *Nat Biotechnol* **29**(8): 742–749.

- Quinlan AR, Hall IM (2010) BEDTools: a flexible suite of utilities for comparing genomic features. *Bioinformatics* **26**(6): 841–842.
- Rinn JL, Chang HY (2012) Genome regulation by long noncoding RNAs. *Annu Rev Biochem* **81**: 145–166.
- Robinson JT, Thorvaldsdottir H, Winckler W, Guttman M, Lander ES, Getz G, Mesirov JP (2011) Integrative genomics viewer. *Nat Biotechnol* **29**(1): 24–26.
- Shen L, Shao NY, Liu X, Maze I, Feng J, Nestler EJ (2013) diffReps: detecting differential chromatin modification sites from ChIP-seq data with biological replicates. *PLoS One* **8**(6): e65598.
- Simmer F, Brinkman AB, Assenov Y, Matarese F, Kaan A, Sabatino L, Villanueva A, Huertas D, Esteller M, Lengauer T, Bock C, Colantuoni V, Altucci L, Stunnenberg HG (2012) Comparative genome-wide DNA methylation analysis of colorectal tumor and matched normal tissues. *Epigenetics* **7**(12): 1355–1367.
- Stroud H, Feng S, Morey Kinney S, Pradhan S, Jacobsen SE (2011) 5-Hydroxymethylcytosine is associated with enhancers and gene bodies in human embryonic stem cells. *Genome Biol* **12**(6): R54.
- Szwagierczak A, Bultmann S, Schmidt CS, Spada F, Leonhardt H (2010) Sensitive enzymatic quantification of 5-hydroxymethylcytosine in genomic DNA. *Nucleic Acids Res* **38**(19): e181.
- Tahiliani M, Koh KP, Shen Y, Pastor WA, Bandukwala H, Brudno Y, Agarwal S, Iyer LM, Liu DR, Aravind L, Rao A (2009) Conversion of 5-methylcytosine to 5-hydroxymethylcytosine in mammalian DNA by MLL partner TET1. *Science* **324**(5929): 930–935.
- Trapnell C, Pachter L, Salzberg SL (2009) TopHat: discovering splice junctions with RNA-Seq. *Bioinformatics* **25**(9): 1105–1111.
- Trimarchi T, Bilal E, Ntziachristos P, Fabbri G, Dalla-Favera R, Tsirigos A, Aifantis I (2014) Genome-wide mapping and characterization of Notch-regulated long noncoding RNAs in acute leukemia. *Cell* **158**(3): 593–606.
- Tsagaratou A, Aijo T, Lio CW, Yue X, Huang Y, Jacobsen SE, Lahdesmaki H, Rao A (2014) Dissecting the dynamic changes of 5-hydroxymethylcytosine in T-cell development and differentiation. *Proc Natl Acad Sci USA* **111**(32): E3306–E3315.
- Ulitsky I, Bartel DP (2013) lincRNAs: genomics, evolution, and mechanisms. *Cell* **154**(1): 26–46.
- Uribe-Lewis S, Stark R, Carroll T, Dunning MJ, Bachman M, Ito Y, Stojic L, Halim S, Vowler SL, Lynch AG, Delatte B, de Bony EJ, Colin L, Defrance M, Krueger F, Silva AL, Ten Hoopen R, Ibrahim AE, Fuks F, Murrell A (2015) 5-hydroxymethylcytosine marks promoters in colon that resist DNA hypermethylation in cancer. *Genome Biol* **16**(1): 69.
- Vaiopoulos AG, Athanasoula K, Papavassiliou AG (2014) Epigenetic modifications in colorectal cancer: molecular insights and therapeutic challenges. *Biochim Biophys Acta* **1842**(7): 971–980.
- White NM, Cabanski CR, Silva-Fisher JM, Dang HX, Govindan R, Maher CA (2014) Transcriptome sequencing reveals altered long intergenic non-coding RNAs in lung cancer. *Genome Biol* **15**(8): 429.
- Whyte WA, Orlando DA, Hnisz D, Abraham BJ, Lin CY, Kagey MH, Rahl PB, Lee TI, Young RA (2013) Master transcription factors and mediator establish super-enhancers at key cell identity genes. *Cell* **153**(2): 307–319.
- Yan X, Hu Z, Feng Y, Hu X, Yuan J, Zhao SD, Zhang Y, Yang L, Shan W, He Q, Fan L, Kandalaft LE, Tanyi JL, Li C, Yuan CX, Zhang D, Yuan H, Hua K, Lu Y, Katsaros D, Huang Q, Montone K, Fan Y, Coukos G, Boyd J, Sood AK, Rebbeck T, Mills GB, Dang CV, Zhang L (2015) Comprehensive genomic characterization of long non-coding RNAs across human cancers. *Cancer Cell* **28**(4): 529–540.
- Yu M, Hon GC, Szulwach KE, Song CX, Zhang L, Kim A, Li X, Dai Q, Shen Y, Park B, Min JH, Jin P, Ren B, He C (2012) Base-resolution analysis of 5-hydroxymethylcytosine in the mammalian genome. *Cell* **149**(6): 1368–1380.
- Zhang LT, Zhang LJ, Zhang JJ, Ye XX, Xie AM, Chen LY, Kang JX, Cai C (2013) Quantification of the sixth DNA base 5-hydroxymethylcytosine in colorectal cancer tissue and C-26 cell line. *Bioanalysis* **5**(7): 839–845.
- Zhang Y, Liu T, Meyer CA, Eickhout J, Johnson DS, Bernstein BE, Nusbaum C, Myers RM, Brown M, Li W, Liu XS (2008) Model-based analysis of ChIP-Seq (MACS). *Genome Biol* **9**(9): R137.

This work is published under the standard license to publish agreement. After 12 months the work will become freely available and the license terms will switch to a Creative Commons Attribution-NonCommercial-Share Alike 4.0 Unported License.

Supplementary Information accompanies this paper on British Journal of Cancer website (<http://www.nature.com/bjc>)